Journal of Siberian Federal University. Chemistry 2 (2015 8) 160-180
~ ~ ~

УДК 546.30

# Thermodynamic Evaluation of Electrochemical Stability of Me – Si Systems (Me = 4th Row Transition Metal)

**Pavel A. Nikolaychuk***
*Chelyabinsk State University*
*129 Bratyev Kashirinykh Str., Chelyabinsk, 454001, Russia*

Received 22.04.2015, received in revised form 16.05.2015, accepted 30.05.2015

*This paper aims to review the studies of electrochemical properties of Me – Si binary systems for scandium, titanium, molybdenum, manganese, iron, cobalt, nickel, copper and zinc from the point of view of chemical thermodynamics. The binary phase diagrams of Me – Si and Me – O systems were considered and thermodynamic properties of metals silicides and oxides at standard conditions were collected. The potential – pH diagrams of Me – Si – $H_2O$ systems at 25 ºC, air pressure of 1 bar and activities of ions in solution equal to 1 mol $l^{-1}$were plotted. The corrosion-electrochemical behavior of studying systems was discussed.*

*Keywords: transition metals, silicides, oxides, chemical and electrochemical stability, potential – pH diagram, corrosion-electrochemical behavior.*

*DOI: 10.17516/1998-2836-2015-8-2-160-180.*


* Corresponding author E-mail address: npa@csu.ru

# Термодинамическая оценка электрохимической устойчивости систем Me – Si (Me = переходный металл 4-го периода)

**П.А. Николайчук**
*Челябинский государственный университет*
*Россия, 454001, Челябинск, ул. Братьев Кашириных, 129*

*Статья представляет собой обзор исследований электрохимических свойств двойных систем Me – Si для скандия, титана, молибдена, марганца, железа, кобальта, никеля, меди и цинка с точки зрения химической термодинамики. Рассмотрены двойные фазовые диаграммы систем Me – Si и Me – O, собраны термодинамические свойства силицидов и оксидов металлов в стандартных условиях. Построены диаграммы потенциал – pH систем Me – Si – $H_2O$ при 25 ºC, давлении воздуха 1 бар и активностях ионов в растворе, равных 1 моль/л. Обсуждается коррозионно-электрохимическое поведение исследуемых систем.*

*Ключевые слова: переходные металлы, силициды, оксиды, химическая и электрохимическая устойчивость, диаграммы потенциал - pH, коррозионно-электрохимическое поведение.*

## Introduction

The silicides of transition 3d-metals are characterized by a very wide variety of physical and chemical properties and an exceptionally wide range of applications in technology. There are conductors with high electroconductivity, semi- and superconductors, metalloids among them. In addition to other things, these compounds have high corrosion resistance; their thermodynamic and electrochemical properties are quite different. The experimental investigations of electrochemical properties of 3d-metals silicides are widely performed [1]. However along with it, a theoretical studying of corrosion-electrochemical behaviour of these systems is also important because it allows complementing and extending experimental data. This paper aims to review the studies of electrochemical properties of Me – Si binary systems for some 4th row d-metals from the point of view of chemical thermodynamics.

All the methods, techniques and approaches used in solving this problem were detailed in monograph [2]. The best carrier of thermodynamic information about possible chemical and electrochemical reactions proceeding in water environments is the diagram of electrochemical equilibrium (electrode potential vs. pH relationship), which allows one to clearly depict the domains of thermodynamic stability of all possible phases and determine the type of system corrosion-electrochemical behavior in certain environmental conditions.

The potential – pH diagrams for pure elements at 25 °C were introduced by M. Pourbaix [3] and are now well known. The procedure of plotting potential – pH diagrams for Me – Si – $H_2O$ systems consists from three steps. At the first step one should study all phase and chemical equilibria in binary Me – Si system at 25 °C basing on its phase diagram, look for reference thermodynamic

data, check they are matched to each other and calculate thermodynamic properties of system components. At the second step one should collect information about all possible oxides and silicates that can be formed during system oxidation, develop the consequence on oxidation processes in oxygen environments and plot the state diagram for Me – Si – O system [2]. At the last step one should consider the ions that can be formed during system oxidation in solutions, possible chemical and electrochemical reactions involving these ions, calculate their electrode potentials and plot the potential – pH diagram. For all systems under consideration the calculations were performed exactly in this order.

The area of electrochemical stability of water has the most importance in analysis of the corrosion behavior of studying systems. The equilibria corresponding to the hydrogen and the oxygen electrodes in atmospheric conditions, which border the area of electrochemical stability of water, are denoted at Figures 1 through 9 by dotted lines. The equations for electrode potentials of these electrodes are presented in Table 1.

In highly reducing conditions metals can form the hydrides. Moreover, the possibility of electrochemical formation of metals nitrides from atmospheric nitrogen was considered in thermodynamic predictions. However, only titanium, nickel and copper hydrides and only a titanium nitride have the domains of thermodynamic stability on potential – pH diagrams. The hydrides and nitrides of other metals either have no thermodynamic data or found to be thermodynamically not stable in aqueous solution.

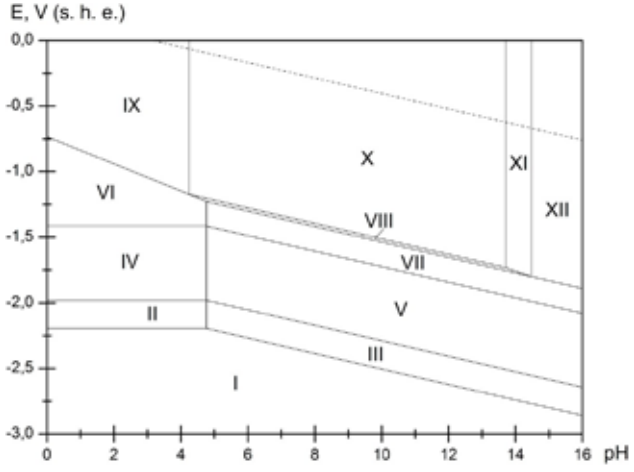


Fig. 1. The potential – pH diagram of Sc – Si – $H_2O$ system at 298 K, air pressure of 1 bar and $a_i$ = 1 mol $l^{-1}$

Table 1. Electrode potentials of the hydrogen and the oxygen electrodes at atmospheric conditions

| Electrode reaction | E, V (s. h. e) |
|---|---|
| $2H^+(aq) + 2e^- \rightleftharpoons H_2(g);\ P_{H_2} \approx 5 \cdot 10^{-7}$ bar | 0.186 – 0.0591 · pH |
| $O_2(g) + 4H^+(aq) + 4e^- \rightleftharpoons H_2O(l);\ P_{O_2} \approx 0.21$ bar | 1.219 – 0.0591 · pH |

It is to be noticed that there are no reliable thermodynamic data on the standard Gibbs energies of formation of some transition metals oxides and silicides. In this case some empirical relationships were used to estimate them.

**Sc – Si system**

According to Sc – Si system phase diagram [4], two scandium silicides – $Sc_5Si_3$ and ScSi – exist is system at standard conditions. The third silicide, $Sc_2Si_3$, exists only at elevated temperatures. All silicides are stoichiometric compounds without any noticeable homogeneity ranges. There are no data on solid solubility of Si in (hcp-Sc) and Sc in (diamond-Si); it is vanishingly small and the components can be treated as insoluble in each other. The standard Gibbs energies of formation of scandium silicides were taken from [5].

Scandium can form only one oxide, $Sc_2O_3$. Its standard Gibbs energy of formation was obtained from [6]. Some scandium silicides exist at elevated temperatures [7] but only thorvertite ($Sc_2Si_2O_7$) remains stable at 298 K. The standard Gibbs energy of formation of this compound was estimated according to $\Delta O^{2-}$ method, proposed by the authors of [8, 9]. It seems that chemical affinity of scandium to oxygen is greater, than that of silicon, and it oxidizes more easily. The oxidation of Sc – Si system in air environments ends with formation of $Sc_2O_3$ and $Sc_2Si_2O_7$ in scandium-rich region and of $Sc_2Si_2O_7$ and $SiO_2$ in silicon-rich region.

In water environments, scandium can form only $Sc^{3+}$cations [10], and silicon can simultaneously exist in form of $SiO_2$, $H_2SiO_3$ and $H_4SiO_4$. However, only orthosilicic acid was considered by means of convenience.

The potential – pH diagram of Sc – Si – $H_2O$ system is plotted at temperature of 298 K, air pressure of 1 bar and activities of ions in solutions, equal to 1 mol $l^{-1}$ and presented at Fig. 1. 12 domains of prevalence of certain phases can be depicted in it: I – Sc (hcp) + $Sc_5Si_3$ + ScSi + Si (dia); II – $Sc^{3+}$ + $Sc_5Si_3$ + ScSi + Si (dia); III – $Sc_2O_3$ + $Sc_5Si_3$ + ScSi + Si (dia); IV – $Sc^{3+}$ + ScSi + Si (dia); V – $Sc_2O_3$ + ScSi + Si (dia); VI – $Sc^{3+}$ + Si (dia); VII – $Sc_2O_3$ + Si (dia); VIII – $Sc_2Si_2O_7$ + Si (dia); IX – $Sc^{3+}$ + $Sc_2Si_2O_7$ + Si (dia); X – $Sc_2Si_2O_7$ + $H_4SiO_4$; XI – $Sc_2Si_2O_7$ + $H_2SiO_4^{2-}$; XII – $Sc_2O_3$ + $Sc_2Si_2O_7$ + Si (dia).

All equilibria in system are realized below the potential of hydrogen electrode. In the area of electrochemical stability of water thermodynamically stable products are $Sc^{3+}$(in acidic solutions), $Sc_2Si_2O_7$ and $H_4SiO_4$. Depending on silicon content in the sample, the passivation film on Sc – Si alloys may consist of thorvertite or orthosilicic acid.

**Ti – Si system**

Titanium silicides are used as cathodes in vacuum arc during the synthesis of super hard nanocrystal coatings [11]. They reveal high corrosion resistance in both reducing and oxidizing environments and can be characterized by stability of the passive state [12].

The following silicides exist in Ti – Si system at 25 °C [4]: $Ti_3Si$, $Ti_5Si_3$, $Ti_5Si_4$, TiSi and $TiSi_2$. It was reported [13] about the compounds $Ti_3Si_4$ and $Ti_6Si_5$, however, there are no confirmations of their existence in other literature. The silicide $Ti_5Si_3$ has wide homogeneity range at elevated temperature, but it can be considered as stoichiometric compound at 25 °C; other silicides do not have any homogeneity ranges. The maximum solid solubility of Si in (hcp-Ti) equals ~3.3 atomic percent

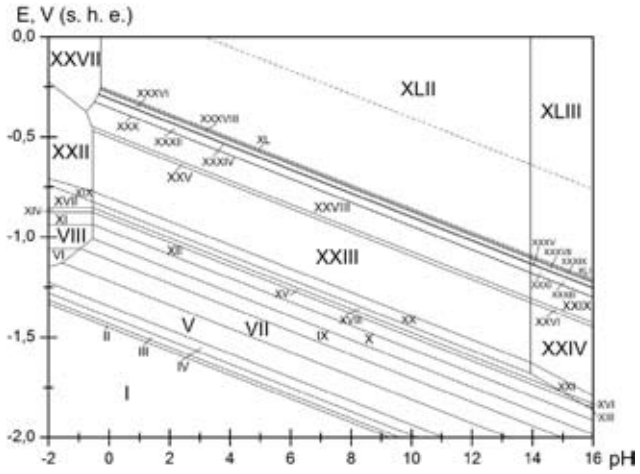


Fig. 2a. The potential – pH diagram of Ti – Si – $H_2O$ system at 298 K, air pressure of 1 bar and $a_i$ = 1 mol $l^{-1}$ without consideration of titanium hydride and nitride

at 1000 °C and only ~0.7 at. % at 800 °C [4], therefore it is vanishingly small at standard temperature and thus can be neglected. The solubility of Ti in (diamond-Si) is about $10^{-17}$ at. % at 1100 °C [14]. The values of standard Gibbs energies of formation of titanium silicides were taken from [15].

The phase diagram of Ti – O system [4] reveals a big number of titanium oxides and suboxides at 298 K – $Ti_6O$, $Ti_3O$, $Ti_2O$, $Ti_3O_2$, TiO, $Ti_2O_3$, $Ti_3O_5$, Magnelli phases $Ti_nO_{2n-1}$ ($4 \le n \le 10$), $TiO_2$. There are no compounds in binary $TiO_2$ – $SiO_2$ system [16]. The standard Gibbs energies of formation of titanium oxides were taken from [17]. Titanium can form anions $Ti^{3+}$ and $TiO^{2+}$ in water solution. No titanate-anions can be formed [18].

The potential – pH diagram of Ti – Si – $H_2O$ system plotted in accordance with Ti – Si – O state diagram [19] is presented at Fig. 2a. It determines 43 domains of thermodynamic stability of certain phases: I – Ti (hcp) + $Ti_3Si$ + $Ti_5Si_3$ + $Ti_5Si_4$ + TiSi + $TiSi_2$ + Si (dia); II – $Ti_6O$ + $Ti_3Si$ + $Ti_5Si_3$ + $Ti_5Si_4$ + TiSi + $TiSi_2$ + Si (dia); III – $Ti_3O$ + $Ti_3Si$ + $Ti_5Si_3$ + $Ti_5Si_4$ + TiSi + $TiSi_2$ + Si (dia); IV – $Ti_2O$ + $Ti_3Si$ + $Ti_5Si_3$ + $Ti_5Si_4$ + TiSi + $TiSi_2$ + Si (dia); V – $Ti_3O_2$ + $Ti_3Si$ + $Ti_5Si_3$ + $Ti_5Si_4$ + TiSi + $TiSi_2$ + Si (dia); VI – $Ti^{3+}$ + $Ti_3Si$ + $Ti_5Si_3$ + $Ti_5Si_4$ + TiSi + $TiSi_2$ + Si (dia); VII – TiO + $Ti_3Si$ + $Ti_5Si_3$ + $Ti_5Si_4$ + TiSi + $TiSi_2$ + Si (dia); VIII – $Ti^{3+}$ + $Ti_5Si_3$ + $Ti_5Si_4$ + TiSi + $TiSi_2$ + Si (dia); IX – TiO + $Ti_5Si_3$ + $Ti_5Si_4$ + TiSi + $TiSi_2$ + Si (dia); X – $Ti_2O_3$ + $Ti_5Si_3$ + $Ti_5Si_4$ + TiSi + $TiSi_2$ + Si (dia); XI – $Ti^{3+}$ + $Ti_5Si_4$ + TiSi + $TiSi_2$ + Si (dia); XII – $Ti_2O_3$ + $Ti_5Si_4$ + TiSi + $TiSi_2$ + Si (dia); XIII – $Ti_2O_3$ + $Ti_5Si_4$ + TiSi + $TiSi_2$ + $H_2SiO_4^{2-}$; XIV – $Ti^{3+}$ + TiSi + $TiSi_2$ + Si (dia); XV – $Ti_2O_3$ + TiSi + $TiSi_2$ + Si (dia); XVI – $Ti_2O_3$ + TiSi + $TiSi_2$ + $H_2SiO_4^{2-}$; XVII – $Ti^{3+}$ + $TiSi_2$ + Si (dia); XVIII – $Ti_2O_3$ + $TiSi_2$ + Si (dia); XIX – $Ti^{3+}$ + $TiSi_2$ + $H_4SiO_4$; XX – $Ti_2O_3$ + $TiSi_2$ + $H_4SiO_4$; XXI – $Ti_2O_3$ + $TiSi_2$ + $H_2SiO_4^{2-}$; XXII – $Ti^{3+}$ + $H_4SiO_4$; XXIII – $Ti_2O_3$ + $H_4SiO_4$; XXIV – $Ti_2O_3$ + $H_2SiO_4^{2-}$; XXV – $Ti_3O_5$ + $H_4SiO_4$; XXVI – $Ti_3O_5$ + $H_2SiO_4^{2-}$; XXVII – $TiO^{2+}$ + $H_4SiO_4$; XXVIII – $Ti_4O_7$ + $H_4SiO_4$; XXIX – $Ti_4O_7$ + $H_2SiO_4^{2-}$; XXX – $Ti_5O_9$ + $H_4SiO_4$; XXXI – $Ti_5O_9$ + $H_2SiO_4^{2-}$; XXXII – $Ti_6O_{11}$ + $H_4SiO_4$; XXXIII – $Ti_6O_{11}$ + $H_2SiO_4^{2-}$; XXXIV – $Ti_7O_{13}$ + $H_4SiO_4$; XXXV – $Ti_7O_{13}$ + $H_2SiO_4^{2-}$; XXXVI – $Ti_8O_{15}$ + $H_4SiO_4$; XXXVII – $Ti_8O_{15}$ + $H_2SiO_4^{2-}$; XXXVIII – $Ti_9O_{17}$ + $H_4SiO_4$; XXXIX – $Ti_9O_{17}$ + $H_2SiO_4^{2-}$; XL – $Ti_{10}O_{19}$ + $H_4SiO_4$; XLI – $Ti_{10}O_{19}$ + $H_2SiO_4^{2-}$; XLII – $TiO_2$ + $H_4SiO_4$; XLIII – $TiO_2$ + $H_2SiO_4^{2-}$.

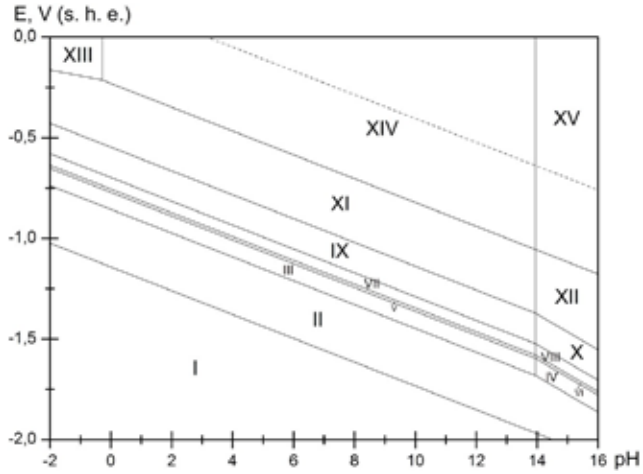


Fig. 2b. The potential – pH diagram of Ti – Si – $H_2O$ system at 298 K, air pressure of 1 bar and $a_i$ = 1 mol $l^{-1}$ with consideration of titanium hydride and nitride

However, titanium has high chemical affinity not only to oxygen but also to hydrogen and nitrogen; therefore electrochemical formation of titanium hydride $TiH_2$ and nitride TiN has to be considered. The diagram taking into account these compounds is presented at Fig. 2b, there are 15 domains of stability of certain phases: I – $TiH_2$ + $Ti_3Si$ + $Ti_5Si_3$ + $Ti_5Si_4$ + TiSi + $TiSi_2$ + Si (dia); II – TiN + $Ti_3Si$ + $Ti_5Si_3$ + $Ti_5Si_4$ + TiSi + $TiSi_2$ + Si (dia); III – TiN + $Ti_3Si$ + $Ti_5Si_3$ + $Ti_5Si_4$ + TiSi + $TiSi_2$ + $H_4SiO_4$; IV – TiN + $Ti_3Si$ + $Ti_5Si_3$ + $Ti_5Si_4$ + TiSi + $TiSi_2$ + $H_2SiO_4^{2-}$; V – TiN + $Ti_3Si$ + $Ti_5Si_3$ + $Ti_5Si_4$ + TiSi + $H_4SiO_4$; VI – TiN + $Ti_3Si$ + $Ti_5Si_3$ + $Ti_5Si_4$ + TiSi + $H_2SiO_4^{2-}$; VII – TiN + $Ti_3Si$ + $Ti_5Si_3$ + $Ti_5Si_4$ + $H_4SiO_4$; VIII – TiN + $Ti_3Si$ + $Ti_5Si_3$ + $Ti_5Si_4$ + $H_2SiO_4^{2-}$; IX – TiN + $Ti_3Si$ + $Ti_5Si_3$ + $H_4SiO_4$; X – TiN + $Ti_3Si$ + $Ti_5Si_3$ + $H_2SiO_4^{2-}$; XI – TiN + $Ti_3Si$ + $H_4SiO_4$; XII – TiN + $Ti_3Si$ + $H_2SiO_4^{2-}$; XIII – $TiO^{2+}$ + $Ti_3Si$ + $H_4SiO_4$; XIV – $TiO_2$ + $Ti_3Si$ + $H_4SiO_4$; XV – $TiO_2$ + $Ti_3Si$ + $H_2SiO_4^{2-}$.

In presence of titanium hydride and nitride all its oxides except $TiO_2$ become thermodynamically unstable. There is no domain of stability of metallic titanium. Moreover, presence of hydride and nitride changes the mechanism and order of titanium silicides oxidation. As can be seen from Fig. 2b, full decomposition of titanium silicides to components is thermodynamically unprofitable process. The presence of silicon in system can stabilize titanium and prevent it from formation of hydride and further oxidation. This can be explained by high strength of Ti – Si covalent bonds [12].

**Mo – Si system**

Molybdenum does not belong to 3d-metals. However, it is the only one metal amongst all 4d-metals that has big importance in metallurgy. Molybdenum silicides are used for making high-temperature thermocouples for measuring temperatures in air up to 1700 ºC, electric resistance heaters, working without protective atmosphere, for creating materials to be used in oxidizing environments. Therefore, this system was included into consideration.

The phase diagram of Mo – Si system [4, 20] assumes the existence of molybdenum silicides $Mo_3Si$, $Mo_5Si_3$ and $MoSi_2$. All these compounds do not have any ranges of nonstoichiometry. The maximum solid solubility of Si in (fcc-Mo) equals ~2.5 atomic percent at 1500 °C and does not

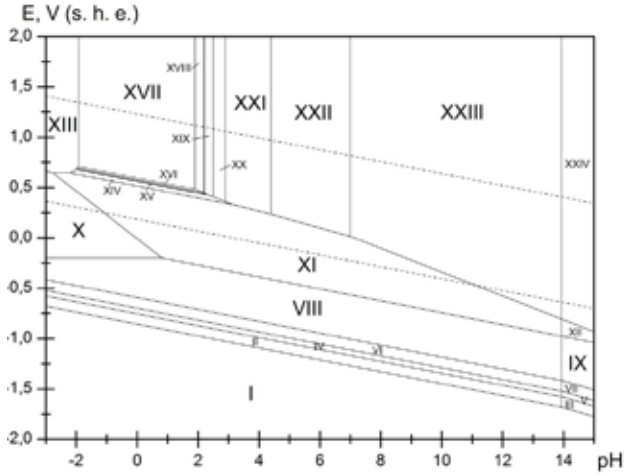


Fig. 3. The potential – pH diagram of Mo – Si – $H_2O$ system at 298 K, air pressure of 1 bar and $a_i$ = 1 mol $l^{-1}$

exceed 1 at. % at 1300 °C [4], therefore it is vanishingly small at standard temperature and thus can be neglected. The values of standard Gibbs energies of formation of molybdenum silicides were taken from [15, 20].

Molybdenum forms stable oxides $MoO_2$, $Mo_4O_{11}$, $Mo_8O_{23}$, $Mo_9O_{26}$, $MoO_3$ and a variety of metastable phases ($Mo_{17}O_{47}$, $Mo_5O_{14}$, $Mo_{18}O_{52}$) [4]. Metastable compounds were not taken into account in thermodynamic calculations. There is no data about the existence of molybdenum silicates. In water solution molybdenum forms the cations $Mo^{3+}$ and $MoO_2^{2+}$ and can be oxidized to various isopolymolybdate-anions with oxidation degree +6 [18, 21 – 23]. According to [24], the following anions are most stable in solution: $H_2Mo_8O_{26}^{2-}$, $HMo_8O_{26}^{3-}$, $Mo_8O_{26}^{4-}$, $H_2Mo_7O_{24}^{4-}$, $Mo_7O_{24}^{6-}$ and $MoO_4^{2-}$. The values of standard Gibbs energies of formation for molybdenum oxides are taken from [25] and the values for molybdate anions are calculated according to data from Pourbaix diagram for molybdenum [26, 27].

The potential – pH diagram of Mo – Si – $H_2O$ system [28] is presented at Fig. 3; 24 domains of predominance of certain phases can be depicted in it: I – Mo (bcc) + $Mo_3Si$ + $Mo_5Si_3$ + $MoSi_2$ + Si (dia) ; II – Mo (bcc) + $Mo_3Si$ + $Mo_5Si_3$ + $MoSi_2$ + $H_4SiO_4$ ; III – Mo (bcc) + $Mo_3Si$ + $Mo_5Si_3$ + $MoSi_2$ + $H_2SiO_4^{2-}$; IV – Mo (bcc) + $Mo_3Si$ + $Mo_5Si_3$ + $H_4SiO_4$ ; V – Mo (bcc) + $Mo_3Si$ + $Mo_5Si_3$ + $H_2SiO_4^{2-}$ ; VI – Mo (bcc) + $Mo_3Si$ + $H_4SiO_4$ ; VII – Mo (bcc) + $Mo_3Si$ + $H_2SiO_4^{2-}$ ; VIII – Mo (bcc) + $H_4SiO_4$ ; IX – Mo (bcc) + $H_2SiO_4^{2-}$ ; X – $Mo^{3+}$ + $H_4SiO_4$ ; XI – $MoO_2$ + $H_4SiO_4$ ; XII – $MoO_2$ + $H_2SiO_4^{2-}$ ; XIII – $MoO_2^{2+}$ + $H_4SiO_4$ ; XIV – $Mo_4O_{11}$ + $H_4SiO_4$ ; XV – $Mo_8O_{23}$ + $H_4SiO_4$ ; XVI – $Mo_9O_{26}$ + $H_4SiO_4$ ; XVII – $MoO_3$ + $H_4SiO_4$ ; XVIII – $H_2Mo_8O_{26}^{2-}$ + $H_4SiO_4$ ; XIX – $HMo_8O_{26}^{3-}$ + $H_4SiO_4$ ; XX – $Mo_8O_{26}^{4-}$ + $H_4SiO_4$ ; XXI – $H_2Mo_7O_{24}^{4-}$ + $H_4SiO_4$ ; XXII – $Mo_7O_{24}^{6-}$ + $H_4SiO_4$ ; XXIII – $MoO_4^{2-}$ + $H_4SiO_4$ ; XXIV – $MoO_4^{2-}$, $H_2SiO_4^{2-}$.

As can be seen from Fig. 3, molybdenum has very narrow domain of active dissolution, because the cations $Mo^{3+}$ and $MoO_2^{2+}$ exist only in strongly acidic environments. However, the domain of the oxide passivation of molybdenum is also quite small, and if the environment becomes more and more alkaline, then the domain of transpassivity (which contains all possible isopolymolybdate forms) becomes more and more broad. Generally, electrochemical stability of molybdenum-silicon alloys is

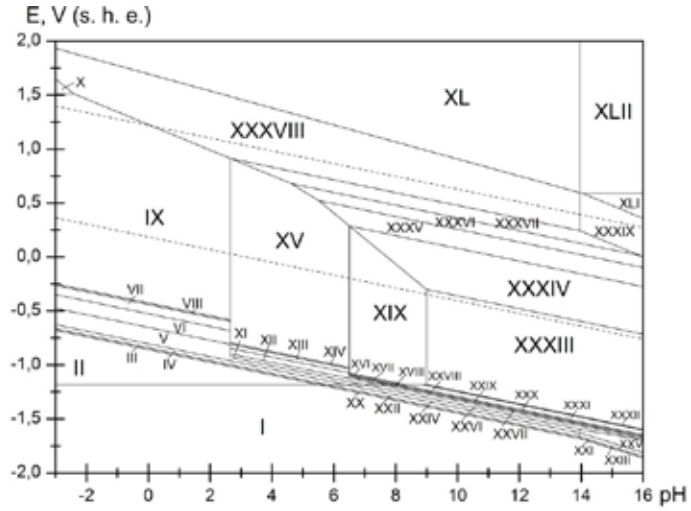


Fig. 4. The potential – pH diagram of Mn – Si – $H_2O$ system at 298 K, air pressure of 1 bar and $a_i$ = 1 mol $l^{-1}$

completely determined by silicon content in them. If it is enough to form a continuous passivation film from $H_4SiO_4$ on alloy surface, then the active oxidation of molybdenum stops.

**Mn – Si system**

Manganese doped by silicon is used in manufacturing of rail and structural steels, in metallurgy as the deoxidizer, as the dopant to alloys based on aluminum, magnesium and copper.

There are seven intermetallic phases in Mn – Si system [4]: $Mn_{11}Si_{19}$, MnSi, $Mn_5Si_3$, $Mn_5Si_2$, $Mn_3Si$, ν-phase ($Mn_9Si_2$) and R-phase ($Mn_6Si$). The first five silicides are stoichiometric phases. ν-phase has a narrow homogeneity range at elevated temperatures but can be considered as stoichiometric compound at standard conditions. R-phase has a noticeable homogeneity range at 25 °C. Moreover, a solid solution of Si in (cubic-Mn) can be formed (α-phase). According to [29], R-phase in equilibrium with α-phase has the composition of $Mn_{0.85}Si_{0.15}$.

The equation for the excess Gibbs energy of α-phase was taken from [30]. Calculated solid solubility of Si in (cubic-Mn) at 25 °C equals 4.56 at. % [30]. Thermodynamic activities of solid solution components are the following: $a_{\mathrm{Mn}(\alpha)} = 0.83$, $a_{\mathrm{Si}(\alpha)} = 3.8 \cdot 10^{-28}$. The solid solubility of Mn in (diamond-Si) is about $10^{-14}$ at. % at 1100 °C [14]. The standard Gibbs energies of formation of manganese silicides were collected from various sources [17, 29, 31 – 33].

Manganese forms the oxides MnO, $Mn_3O_4$, $Mn_2O_3$, $MnO_2$ and $Mn_2O_7$ though the last one is not stable in water solutions. There are two manganese silicates at 25 °C – $MnSiO_3$ and $Mn_2SiO_4$ [34]. The compound $Mn_7SiO_{12}$ exist only at elevated temperatures [35]. The ions $Mn^{2+}$, $Mn^{3+}$, $MnO_4^{2-}$ and $MnO_4^-$ exist in water solutions. The standard Gibbs energies of formation of manganese oxides, silicates and ions were taken from [17].

The potential – pH diagram of Mn – Si – $H_2O$ system [30] is presented at Fig. 4. 42 domains of thermodynamic stability of certain phases can be depicted in the diagram: I – α-phase (Mn) + R-phase ($Mn_{0.85}Si_{0.15}$) + ν-phase ($Mn_9Si_2$) + $Mn_3Si$ + $Mn_5Si_2$ + $Mn_5Si_3$ + MnSi + $Mn_{11}Si_{19}$ + Si (dia); II – $Mn^{2+}$ + $Mn_{0.85}Si_{0.15}$ + $Mn_9Si_2$ + $Mn_3Si$ + $Mn_5Si_2$ + $Mn_5Si_3$ + MnSi + $Mn_{11}Si_{19}$ + Si (dia); III – $Mn^{2+}$ + $Mn_{0.85}Si_{0.15}$

+ $Mn_9Si_2$ + $Mn_3Si$ + $Mn_5Si_2$ + $Mn_5Si_3$ + MnSi + $Mn_{11}Si_{19}$ + $H_4SiO_4$; IV – $Mn^{2+}$ + $Mn_{0.85}Si_{0.15}$ + $Mn_9Si_2$ + $Mn_3Si$ + $Mn_5Si_2$ + $Mn_5Si_3$ + MnSi + $H_4SiO_4$; V – $Mn^{2+}$ + $Mn_{0.85}Si_{0.15}$ + $Mn_9Si_2$ + $Mn_3Si$ + $Mn_5Si_2$ + $Mn_5Si_3$ + $H_4SiO_4$; VI – $Mn^{2+}$ + $Mn_{0.85}Si_{0.15}$ + $Mn_9Si_2$ + $Mn_3Si$ + $Mn_5Si_2$ + $H_4SiO_4$; VII – $Mn^{2+}$ + $Mn_{0.85}Si_{0.15}$ + $Mn_9Si_2$ + $Mn_3Si$ + $H_4SiO_4$; VIII – $Mn^{2+}$ + $Mn_{0.85}Si_{0.15}$ + $Mn_9Si_2$ + $H_4SiO_4$; IX – $Mn^{2+}$ + $Mn_{0.85}Si_{0.15}$ + $H_4SiO_4$; X – $Mn^{3+}$ + $Mn_{0.85}Si_{0.15}$ + $H_4SiO_4$; XI – $Mn^{2+}$ + $Mn_{0.85}Si_{0.15}$ + $Mn_9Si_2$ + $Mn_3Si$ + $Mn_5Si_2$ + $Mn_5Si_3$ + $MnSiO_3$; XII – $Mn^{2+}$ + $Mn_{0.85}Si_{0.15}$ + $Mn_9Si_2$ + $Mn_3Si$ + $Mn_5Si_2$ + $MnSiO_3$; XIII – $Mn^{2+}$ + $Mn_{0.85}Si_{0.15}$ + $Mn_9Si_2$ + $Mn_3Si$ + $MnSiO_3$; XIV – $Mn^{2+}$ + $Mn_{0.85}Si_{0.15}$ + $Mn_9Si_2$ + $MnSiO_3$; XV – $Mn^{2+}$ + $Mn_{0.85}Si_{0.15}$ + $MnSiO_3$; XVI – $Mn^{2+}$ + $Mn_{0.85}Si_{0.15}$ + $Mn_9Si_2$ + $Mn_3Si$ + $Mn_5Si_2$ + $Mn_2SiO_4$; XVII – $Mn^{2+}$ + $Mn_{0.85}Si_{0.15}$ + $Mn_9Si_2$ + $Mn_3Si$ + $Mn_2SiO_4$; XVIII – $Mn^{2+}$ + $Mn_{0.85}Si_{0.15}$ + $Mn_9Si_2$ + $Mn_2SiO_4$; XIX – $Mn^{2+}$ + $Mn_{0.85}Si_{0.15}$ + $Mn_2SiO_4$; XX – α + $Mn_{0.85}Si_{0.15}$ + $Mn_9Si_2$ + $Mn_3Si$ + $Mn_5Si_2$ + $Mn_5Si_3$ + MnSi + $Mn_{11}Si_{19}$ + $H_4SiO_4$; XXI – α + $Mn_{0.85}Si_{0.15}$ + $Mn_9Si_2$ + $Mn_3Si$ + $Mn_5Si_2$ + $Mn_5Si_3$ + MnSi + $Mn_{11}Si_{19}$ + $H_2SiO_4^{2-}$; XXII – α + $Mn_{0.85}Si_{0.15}$ + $Mn_9Si_2$ + $Mn_3Si$ + $Mn_5Si_2$ + $Mn_5Si_3$ + MnSi + $H_4SiO_4$; XXIII – α + $Mn_{0.85}Si_{0.15}$ + $Mn_9Si_2$ + $Mn_3Si$ + $Mn_5Si_2$ + $Mn_5Si_3$ + MnSi + $H_2SiO_4^{2-}$; XXIV – α + $Mn_{0.85}Si_{0.15}$ + $Mn_9Si_2$ + $Mn_3Si$ + $Mn_5Si_2$ + $Mn_5Si_3$ + $H_4SiO_4$; XXV – α + $Mn_{0.85}Si_{0.15}$ + $Mn_9Si_2$ + $Mn_3Si$ + $Mn_5Si_2$ + $Mn_5Si_3$ + $H_2SiO_4^{2-}$; XXVI – α + $Mn_{0.85}Si_{0.15}$ + $Mn_9Si_2$ + $Mn_3Si$ + $Mn_5Si_2$ + $Mn_5Si_3$ + $MnSiO_3$; XXVII – α + $Mn_{0.85}Si_{0.15}$ + $Mn_9Si_2$ + $Mn_3Si$ + $Mn_5Si_2$ + $MnSiO_3$; XXVIII – α + $Mn_{0.85}Si_{0.15}$ + $Mn_9Si_2$ + $Mn_3Si$ + $Mn_5Si_2$ + $Mn_2SiO_4$; XXIX – α + $Mn_{0.85}Si_{0.15}$ + $Mn_9Si_2$ + $Mn_3Si$ + $Mn_2SiO_4$; XXX – α + $Mn_{0.85}Si_{0.15}$ + $Mn_9Si_2$ + $Mn_3Si$ + $Mn_2SiO_4$ + MnO; XXXI – α + $Mn_{0.85}Si_{0.15}$ + $Mn_9Si_2$ + $Mn_2SiO_4$ + MnO; XXXII – α + $Mn_{0.85}Si_{0.15}$ + $Mn_2SiO_4$ + MnO; XXXIII – $Mn_{0.85}Si_{0.15}$ + $Mn_2SiO_4$ + MnO; XXXIV – $Mn_{0.85}Si_{0.15}$ + $Mn_2SiO_4$ + $Mn_3O_4$; XXXV – $Mn_{0.85}Si_{0.15}$ + $MnSiO_3$ + $Mn_3O_4$; XXXVI – $Mn_{0.85}Si_{0.15}$ + $MnSiO_3$ + $Mn_2O_3$; XXXVII – $Mn_{0.85}Si_{0.15}$ + $MnSiO_3$ + $MnO_2$; XXXVIII – $Mn_{0.85}Si_{0.15}$ + $MnO_2$ + $H_4SiO_4$; XXXIX – $Mn_{0.85}Si_{0.15}$ + $MnO_2$ + $H_2SiO_4^{2-}$; XL – $Mn_{0.85}Si_{0.15}$ + $H_4SiO_4$ + $MnO_4^-$; XLI – $Mn_{0.85}Si_{0.15}$ + $MnO_4^{2-}$, $H_2SiO_4^{2-}$; XLII – $Mn_{0.85}Si_{0.15}$ + $MnO_4^-$, $H_2SiO_4^{2-}$.

The corrosion-electrochemical behavior of manganese-silicon alloys is determined by the acidity of environment and the value of equilibrium potential. In acidic environments the selective corrosion of manganese takes place and it forms the cations $Mn^{2+}$ and silicon from alloy is oxidized to silicic acid. In neutral and alkaline environments oxidation can end with formation of passivation film consisting of silicates $Mn_2SiO_4$ or $MnSiO_3$.

**Fe – Si system**

Iron–silicon is a very important binary system for metallurgy. Iron silicides are perspective materials; they are well-known for their unusual magnetic, optical and thermodynamic properties [36]. Iron-silicon alloys can be found in Earth's core [37], they are using in technology as thin films [38] and nanowires [39]. Moreover, many important ternary and multicomponent systems, including Fe – Si binary system are of great interest to the researcher.

According to the Fe – Si phase diagram [4], several intermetallic phases exist in system: $Fe_3Si_7$, $FeSi_2$, FeSi, $Fe_5Si_3$ and $Fe_2Si$. But only $FeSi_2$ and FeSi are thermodynamically stable at standard conditions. FeSi has a narrow homogeneity range [4, 40], from $FeSi_{0.961}$ to $FeSi_{1.033}$, which does not depend on temperature. The solid solubility of Si in (bcc-Fe) is equal to about 25 atomic percent at ambient temperatures and silicon can form three types of solutions. The first one is the disordered phase, in which only short range ordering exists (α-phase), two others have long range atomic ordering – $\alpha_2$-phase and $\alpha_1$-phase. Additionally, a miscibility gap exists between $\alpha_2$ and $\alpha_1$ phases. Moreover, a fully ordered $\alpha_1$-

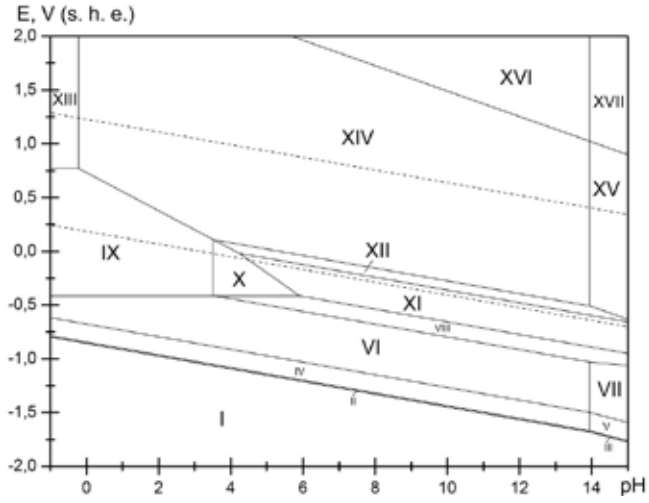


Fig. 5. The potential – pH diagram of Fe – Si – $H_2O$ system at 298 K, air pressure of 1 bar and $a_i$ = 1 mol $l^{-1}$

phase is often treated as independent compound $Fe_3Si$ [41]. The expression for the excess Gibbs energy of α-phase was taken from [42]. The activities of the components of solid solution corresponding to maximum silicon solubility in $\alpha_1$-phase are the following: $a_{Fe(\alpha_1)} = 0.473$ and $a_{Si(\alpha_1)} = 5.5 \cdot 10^{-20}$ meaning strong negative deviations from ideal behaviour. The solid solubility of silicon in disordered α-phase at 25 °C is about ~11 at. %. The activities of the components in this solution are equal to $a_{Fe(\alpha)} = 0.13$, $a_{Si(\alpha)} = 5.0 \cdot 10^{-20}$. The solubility of Fe in (diamond-Si) is about $10^{-17}$ at. % at 1100 °C [14]. The standard Gibbs energies of formation of iron silicides were collected from [17, 42 – 45].

Iron can form the following oxides: FeO, $Fe_3O_4$ and $Fe_2O_3$. However, FeO is not thermodynamically stable at temperatures below 570 °C [9]. $Fe_3O_4$ and $Fe_2O_3$ have noticeable homogeneity ranges at elevated temperatures but they are stoichiometric compounds at 25 °C. Only one ternary compound exists in Fe – Si – O system, it is $Fe_2SiO_4$ [46]. Another compound, $FeSiO_3$, exists only at elevated temperatures and pressures [47]. A solid solution of $Fe_3O_4$ in $Fe_2SiO_4$ can be formed [48] and its maximum solubility at 25 °C equals $6.85 \cdot 10^{-5}$ at. %. In addition, up to $1.54 \cdot 10^{-3}$ at. % of $SiO_2$ can be dissolved in $Fe_2O_3$ [48]. The values of standard Gibbs energies of formation of iron oxides were obtained from [17, 25, 49], the values for $Fe_2SiO_4$ – from [46, 50, 51].

The following ions of iron can be formed in water solution: $Fe^{2+}$, $Fe^{3+}$, $FeO_4^{2-}$. The potential – pH diagram of Fe – Si – $H_2O$ is presented at Fig. 5, and 17 domains of stability of certain phases can be depicted in it: I – α-phase (Fe) + $FeSi_x$ + $FeSi_2$ + Si (dia); II – α + $FeSi_x$ + $FeSi_2$ + $H_4SiO_4$; III – α + $FeSi_x$ + $FeSi_2$ + $H_2SiO_4^{2-}$; IV – α + $FeSi_x$ + $H_4SiO_4$; V – α + $FeSi_x$ + $H_2SiO_4^{2-}$; VI – α + $H_4SiO_4$; VII – α + $H_2SiO_4^{2-}$; VIII – α + $Fe_2SiO_4$; IX – $Fe^{2+}$ + $H_4SiO_4$; X – $Fe^{2+}$ + $Fe_2SiO_4$; XI – [$Fe_2$(Fe, Si)$O_4$] + $Fe_2SiO_4$; XII – $Fe_2O_3$ + $Fe_2SiO_4$; XIII – $Fe^{3+}$ + $H_4SiO_4$; XIV – $Fe_2O_3$ + $H_4SiO_4$; XV – $Fe_2O_3$ + $H_2SiO_4^{2-}$; XVI – $FeO_4^{2-}$ + $H_4SiO_4$; XVII – $FeO_4^{2-}$, $H_2SiO_4^{2-}$.

In contrast to other systems, silicon plays a minor role in corrosion properties of iron silicides. The domain of thermodynamic stability of $Fe_2SiO_4$ lies almost below the potential of hydrogen electrode. The passivation film consists of $Fe_2O_3$ or $H_2SiO_4$ depending on silicon concentration.

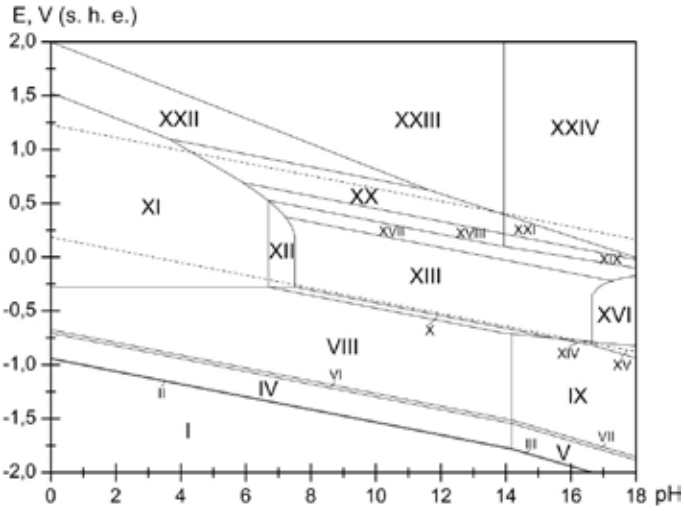


Fig. 6. The potential – pH diagram of Co – Si – $H_2O$ system at 298 K, air pressure of 1 bar and $a_i$ = 1 mol $l^{-1}$

**Co – Si system**

Cobalt and silicon are the basic components of cobalt-based amorphous alloys [52], which are of interest to the researchers due to their unusual magnetic, mechanical, electric properties as well as high corrosion resistance.

The compounds $Co_2Si$, CoSi and $CoSi_2$ exist in Co – Si system at 25 °C [4, 53]. Moreover, a solid solution of Si in (hcp-Co) (ε-phase) exists in cobalt-rich region of Co – Si phase diagram. The expression for the excess Gibbs energy of this phase was provided in paper [42]. Calculated maximum solid solubility of silicon at 25 °C [54] equals 10.7 at. %, thermodynamic activities of this saturated solid solution are the following: $a_{Co(\varepsilon)} = 0.27$, $a_{Si(\varepsilon)} = 4 \cdot 10^{-16}$. The solubility of Co in (diamond-Si) is about $10^{-17}$ at. % at 1000 °C [14]. The values of standard Gibbs energies of formation of cobalt silicides were collected from [17, 25, 42, 53].

Cobalt can form a variety of oxides – CoO, $Co_3O_4$, $Co_2O_3$ and $CoO_2$; the first two ones have a noticeable homogeneity range, which covers the compositions from CoO to $CoO_{1.07}$ for "CoO" phase and from $CoO_{1.31}$ to $CoO_{1.41}$ for "$Co_3O_4$" phase [4, 55]. Only one ternary compound, $Co_2SiO_4$, exists in Co – Si – O system [56]. The values of Gibbs energies of formation of cobalt oxides and silicides were obtained from [17, 25, 55].

Cobalt can form the cation $Co^{2+}$ and the anions $HCoO_2^-$ and $CoO_4^{2-}$ in water solution. The potential – pH diagram of Co – Si – $H_2O$ system [54] is presented at Fig. 6.

24 domains of stability of certain phases can be depicted at the diagram: I – ε-phase (Co) + $Co_2Si$ + CoSi + $CoSi_2$ + Si (dia); II – ε + $Co_2Si$ + CoSi + $CoSi_2$ + $H_4SiO_4$; III – ε-фаза(Co) + $Co_2Si$ + CoSi + $CoSi_2$ + $H_2SiO_4^{2-}$; IV – ε + $Co_2Si$ + CoSi + $H_4SiO_4$; V – ε + $Co_2Si$ + CoSi + $H_2SiO_4^{2-}$; VI – ε + $Co_2Si$ + $H_4SiO_4$; VII – ε + $Co_2Si$ + $H_2SiO_4^{2-}$; VIII – ε + $H_4SiO_4$; IX – ε + $H_2SiO_4^{2-}$; X – ε + $Co_2SiO_4$; XI – $H_4SiO_4$ + $Co^{2+}$; XII – $Co_2SiO_4$ + $Co^{2+}$; XIII – $Co_2SiO_4$ + "CoO"; XIV – "CoO" + $H_2SiO_4^{2-}$; XV – $HCoO_2^-$, $H_2SiO_4^{2-}$; XVI – $Co_2SiO_4$ + $HCoO_2^-$; XVII – $Co_2SiO_4$ + "$Co_3O_4$"; XVIII – "$Co_3O_4$" + $H_4SiO_4$; XIX – "$Co_3O_4$" + $H_2SiO_4^{2-}$; XX – $Co_2O_3$ + $H_4SiO_4$; XXI – $Co_2O_3$ + $H_2SiO_4^{2-}$; XXII – $CoO_2$ + $H_4SiO_4$; XXIII – $H_4SiO_4$ + $CoO_4^{2-}$; XXIV – $CoO_4^{2-}$, $H_2SiO_4^{2-}$.

If the content of silicon in system is sufficient to form a continuous layer of cobalt silicate, it becomes a primarily passivation film. Otherwise, the protecting film consisting of cobalt oxides "CoO" and "$Co_3O_4$" would be formed. In strongly acidic environments, where cobalt dissolves to form $Co^{2+}$, the oxidation film consists of orthosilicic acid.

**Ni – Si system**

According to the Ni – Si phase diagram [4, 57], several phases exist in system at standard conditions. There are six intermediate phases: $\beta_1$-phase ($Ni_3Si$), γ-phase ($Ni_5Si_2$ or $Ni_{31}Si_{12}$ [58]), δ-phase ($Ni_2Si$), ε-phase ($Ni_3Si_2$), NiSi and $NiSi_2$. Although almost all nickel silicides have a narrow homogeneity ranges at 800 ºC [57], they can be treated as stoichiometric phases at standard temperature. The solubility of Ni in (diamond-Si) does not exceed $10^{-16}$ at. % at 800 °C [14]. At the nickel-rich part of the system, the solid solution of Si in (fcc-Ni) can be formed (α-phase). There is no published information about silicon maximum solid solubility at 25 ºC, but it is relatively high (more that 10 atomic percent) at 1000 ºC [4]. Most CALPHAD assessments of Ni – Si system [57, 59 – 61] consider $\beta_1$-phase as an ordered solid solution and use an order-disorder contribution model [62] for its Gibbs energy function. Moreover, they use sublattice model [63] for Gibbs energy function of α-phase. But, since $\beta_1$-phase can be assumed as stoichiometric and composition invariant at standard temperature, there is no necessity to pay attention on order-disorder transformations in it and use such complicated thermodynamic models. Therefore, simpler thermodynamics model was used to describe the excess Gibbs energy of α-phase [64]. Calculated solid solubility of Si in (fcc-Ni) at 25 ºC equals 2.5 at. %. The activities of solid solution components are the following: $a_{\mathrm{Ni}(\alpha)} = 0.927$, $a_{\mathrm{Si}(\alpha)} = 9 \cdot 10^{-36}$.

It is well known, that nickel monoxide (NiO) and higher nickel oxides ($Ni_2O_3$, $NiO_2$) can form a continuous series of solid solutions, which corresponds to a variable composition phase $NiO_x$ [65].

A single ternary compound exist in Ni – Si – O system, it is nickel orthosilicate $Ni_2SiO_4$ [46]. The values of standard Gibbs energies of formation of nickel silicides and nickel silicate were collected from various sources and analyzed by the authors of [64]. The expression for the standard Gibbs energy of formation of phase $NiO_x$ was also proposed in [64].

Nickel can form the following ions in water solutions: $Ni^{2+}$, $HNiO_2^-$ and $NiO_4^{2-}$ [2]. The potential – pH diagram of Ni – Si – $H_2O$ system [64] is presented at Fig. 7a. 24 domains of thermodynamic stability of certain phases can be depicted at the diagram: I – α-phase (Ni) + $Ni_3Si$ + $Ni_5Si_2$ + $Ni_2Si$ + $Ni_3Si_2$ + NiSi + $NiSi_2$ + Si (dia); II – α + $Ni_3Si$ + $Ni_5Si_2$ + $Ni_2Si$ + $Ni_3Si_2$ + NiSi + $NiSi_2$ + $H_4SiO_4$; III – α + $Ni_3Si$ + $Ni_5Si_2$ + $Ni_2Si$ + $Ni_3Si_2$ + NiSi + $NiSi_2$ + $H_2SiO_4^{2-}$; IV – α + $Ni_3Si$ + $Ni_5Si_2$ + $Ni_2Si$ + $Ni_3Si_2$ + NiSi + $H_4SiO_4$; V – α + $Ni_3Si$ + $Ni_5Si_2$ + $Ni_2Si$ + $Ni_3Si_2$ + NiSi + $H_2SiO_4^{2-}$; VI – α + $Ni_3Si$ + $Ni_5Si_2$ + $Ni_2Si$ + $Ni_3Si_2$ + $H_4SiO_4$; VII – α + $Ni_3Si$ + $Ni_5Si_2$ + $Ni_2Si$ + $Ni_3Si_2$ + $H_2SiO_4^{2-}$; VIII – α + $Ni_3Si$ + $Ni_5Si_2$ + $Ni_2Si$ + $H_4SiO_4$; IX – α + $Ni_3Si$ + $Ni_5Si_2$ + $Ni_2Si$ + $H_2SiO_4^{2-}$; X – α + $Ni_3Si$ + $Ni_5Si_2$ + $H_4SiO_4$; XI – α + $Ni_3Si$ + $Ni_5Si_2$ + $H_2SiO_4^{2-}$; XII – α + $Ni_3Si$ + $H_4SiO_4$; XIII – α + $Ni_3Si$ + $H_2SiO_4^{2-}$; XIV – α + $H_4SiO_4$; XV – α + $H_2SiO_4^{2-}$; XVI – α + $Ni_2SiO_4$; XVII – $Ni^{2+}$ + $H_4SiO_4$; XVIII – $Ni^{2+}$ + $Ni_2SiO_4$; XIX – $NiO_x$ + $Ni_2SiO_4$; XX – $HNiO_2^-$ + $Ni_2SiO_4$; XXI – $NiO_x$ + $H_4SiO_4$; XXII – $NiO_x$ + $H_2SiO_4^{2-}$; XXIII – $NiO_4^{2-}$ + $H_4SiO_4$; XXIV – $NiO_4^{2-}$, $H_2SiO_4^{2-}$.

In addition nickel can form the hydride $Ni_2H$ [66]. The possibilities of electrochemical reduction of nickel to its hydride are discussed in [67]. The information about the Gibbs energy of formation for

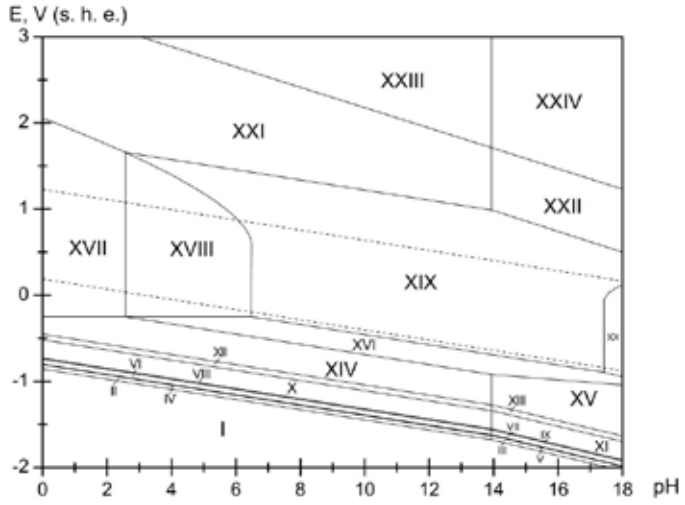


Fig. 7a. The potential – pH diagram of Ni – Si – $H_2O$ system at 298 K, air pressure of 1 bar and $a_i$ = 1 mol $l^{-1}$ without consideration of nickel hydride

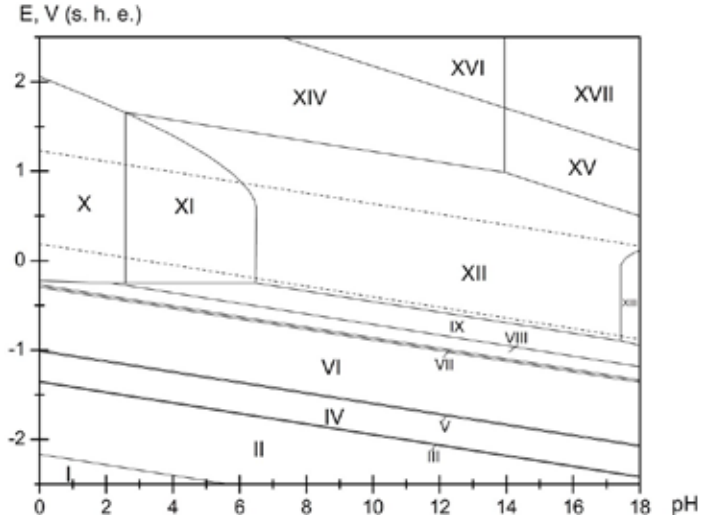


Fig. 7b. The potential – pH diagram of Ni – Si – $H_2O$ system at 298 K, air pressure of 1 bar and $a_i$ = 1 mol $l^{-1}$ with consideration of nickel hydride

nickel hydride $Ni_2H$ was taken from paper [68]. The potential – pH diagram of Ni – Si – $H_2O$ system with consideration of nickel hydride is presented at Fig. 7b.

17 domains of thermodynamic stability of certain phases can be depicted at the diagram: I – $Ni_2H$ + $Ni_3Si$ + $Ni_5Si_2$ + $Ni_2Si$ +$Ni_3Si_2$ + NiSi + $NiSi_2$ + Si (dia); II – $Ni_2H$ + $Ni_3Si$ + $Ni_5Si_2$ + $Ni_2Si$ + $Ni_3Si_2$ + NiSi + $NiSi_2$;III – $Ni_2H$ + $Ni_3Si$ + $Ni_5Si_2$ + $Ni_2Si$ + $Ni_3Si_2$ + NiSi; IV – $Ni_2H$ + $Ni_3Si$ + $Ni_5Si_2$ + $Ni_2Si$ + $Ni_3Si_2$; V – $Ni_2H$ + $Ni_3Si$ + $Ni_5Si_2$ + $Ni_2Si$; VI – $Ni_2H$ + $Ni_3Si$ + $Ni_5Si_2$; VII – $Ni_2H$ + $Ni_3Si$; VIII – $Ni_2H$ + $Ni_2SiO_4$; IX – Ni (α) + $Ni_2SiO_4$; X – $Ni^{2+}$ + $H_4SiO_4$; XI – $Ni^{2+}$ + $Ni_2SiO_4$; XII – $NiO_x$ + $Ni_2SiO_4$; XIII –

$HNiO_2^- + Ni_2SiO_4$; XIV – $NiO_x + H_4SiO_4$; XV – $NiO_x + H_2SiO_4^{2-}$; XVI – $NiO_4^{2-} + H_4SiO_4$; XVII – $NiO_4^{2-} + H_2SiO_4^{2-}$.

In presence of nickel hydride orthosilicic acid becomes thermodynamically unstable and the mechanism of nickel silicides decomposition slightly changes.

Generally, the corrosion-electrochemical behaviour of iron, cobalt and nickel silicides is very similar. In acidic environments the passivation layer on Fe – Si, Co – Si и Ni – Si system alloys will consist of pure $H_4SiO_4$, if there will be no $F^-$ ions in solution, and metal from alloys will form the cations $Fe^{2+}$, $Co^{2+}$ and $Ni^{2+}$, respectively. In neutral and alkaline environments three cases can be considered. If silicon content in alloys is high, it will be sufficient to form a persistent passivation layer of $SiO_2 \cdot 2H_2O$ on the surface. At lower silicon content in alloy it will be sufficient only to form a persistent layer of silicates $Fe_2SiO_4$, $Co_2SiO_4$ or $Ni_2SiO_4$. If silicon content in alloy is very low, the protective film will consist from corresponding metal oxides, and silicon in form of local inclusions of silicates will be present in its inner layer.

**Cu – Si system**

Alloying of copper alloys with silicon allows increasing their durability, plasticity, improving their mechanical, foundry and anticorrosive properties. Siliceous bronzes and brasses are very cheap substitutes for tin bronzes. In addition, silicon can be included in other copper-based alloys with aluminum, nickel, manganese. Therefore, Cu – Si system is a very important binary system for the metallurgy and chemical technology.

In Cu – Si system 25 ºC the existence of the following copper silicides was approved [4, 69]: $Cu_{56}Si_{11}$ (γ-phase), $Cu_{15}Si_4$ (ε-phase) and $Cu_{19}Si_6$ (η''-phase). Despite all copper silicides have, in greater or lesser degree, the homogeneity range, it is negligibly small at the standard temperature, and the silicides can be assumed as daltonides. Additionally, a solid solution of Si in (fcc-Cu) (α-phase) exists in copper-rich copper of system. The expression for the excess Gibbs energy of α-phase was taken from [69]. The calculated silicon maximum solid solubility in α-phase at standard temperature slightly exceeds 4 at. %. Thermodynamic activities of the components of saturated solid solution are the following: $a_{Cu(\alpha)} = 0.92$, $a_{Si(\alpha)} = 5.6 \cdot 10^{-8}$. The standard Gibbs energies of formation of copper silicides were estimated in [70].

In addition to well known oxides $Cu_2O$ and CuO copper can also form a $Cu_2O_3$ compound [71]. Only one ternary compound exists in Cu – Si – O ternary system, it is $CuSiO_3$ [46]. The standard Gibbs energies of formation of copper oxides and silicate were collected from [17, 25, 71].

Copper in water solution can form the the cation $Cu^{2+}$ and the anions $HCuO_2^-$ and $CuO_2^{2-}$, however $HCuO_2^-$ is stable only at low concentrations of copper species in solution [70]. Despite copper hydride $CuH_{0.8}$ is not stable in air, it was shown [72 – 74], that it can be obtained during copper electrochemical reduction. The value of standard Gibbs energy of formation for copper hydride was determined by the authors of [75, 76].

The potential – pH diagram of Cu – Si – $H_2O$ system [70] is presented at Fig. 8 and it determines 22 domains of prevalence of certain phases: I – $CuH_{0.8}$ + γ-phase ($Cu_{56}Si_{11}$) + ε-phase ($Cu_{15}Si_4$) + η''-phase ($Cu_{19}Si_6$) + Si (dia); II – $CuH_{0.8}$ + γ + ε + η'' + $H_4SiO_4$; III – $CuH_{0.8}$ + γ + ε + η'' + $H_2SiO_4^{2-}$; IV – α-phase (Cu) + γ + ε + η'' + $H_4SiO_4$; V – α + γ + ε + η'' + $H_2SiO_4^{2-}$;

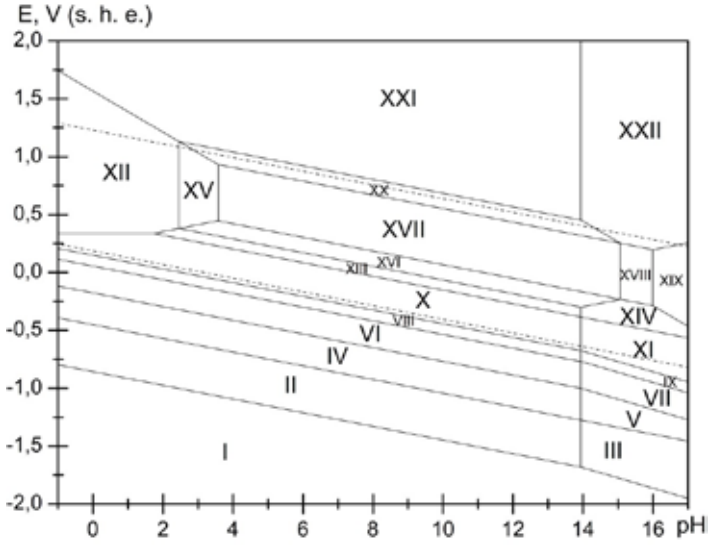


Fig. 8. The potential – pH diagram of Cu – Si – $H_2O$ system at 298 K, air pressure of 1 bar and $a_i$ = 1 mol $l^{-1}$

VI – α + γ + ε + $H_4SiO_4$; VII – α + γ + ε + $H_2SiO_4^{2-}$; VIII – α + γ + $H_4SiO_4$; IX – α + γ + $H_2SiO_4^{2-}$; X – α + $H_4SiO_4$; XI – α + $H_2SiO_4^{2-}$; XII – $Cu^{2+}$ + $H_4SiO_4$; XIII – $Cu_2O$ + $H_4SiO_4$; XIV – $Cu_2O$ + $H_2SiO_4^{2-}$; XV – $Cu^{2+}$ + $CuSiO_3$; XVI – $Cu_2O$ + $CuSiO_3$; XVII – CuO + $CuSiO_3$; XVIII – CuO + $H_2SiO_4^{2-}$; XIX – $CuO_2^{2-}$ + $H_2SiO_4^{2-}$; XX – $Cu_2O_3$ + $CuSiO_3$; XXI – $Cu_2O_3$ + $H_4SiO_4$; XXII – $Cu_2O_3$ + $H_2SiO_4^{2-}$.

The electrochemical behaviour of Cu – Si system strongly differs depending on the composition of system and solution. Many compounds including copper and silicon oxides, copper silicate and various ionic species have the domains of prevalence in the area of electrochemical stability of water. The composition of passivation layer on Cu – Si alloys will vary depending on environmental conditions.

**Zn – Si system**

There are no intermediate compounds in Zn – Si system. Moreover, hcp-Zn and diamond-Si are insoluble in each other and form only mechanical mixture at ambient temperature [4].

Zinc can form two oxides, ZnO and $ZnO_2$ [77]. One zinc silicate, $ZnSiO_3$ can be formed in Zn – Si – O system [78]. Another compound, willemite ($Zn_2SiO_4$) can be formed only at high temperatures or high pressures [46]. The standard Gibbs energies of formation of zinc oxides and silicate were collected from [17, 25, 79]. Zinc in water solution can form the cation $Zn^{2+}$ and the anions $HZnO_2^-$ and $ZnO_2^{2-}$, however $HZnO_2^-$ is stable only at low concentrations of zinc species in solution [80].

The potential – pH diagram of Zn – Si – $H_2O$ system is presented at Fig. 9. There are 12 domains corresponding to stability of certain phases: I – Zn (hcp) + Si (dia); II – Zn (hcp) + $H_4SiO_4$; III – Zn (hcp) + $H_2SiO_4^{2-}$; IV – Zn (hcp) + $ZnSiO_3$; V – $Zn^{2+}$ + $H_4SiO_4$; VI – $Zn^{2+}$ + $ZnSiO_3$; VII – ZnO + $ZnSiO_3$; VIII – $ZnO_2^{2-}$ + $ZnSiO_3$; XI – $ZnO_2^{2-}$, $H_2SiO_4^{2-}$; X – $ZnO_2$ + $ZnSiO_3$; XI – $ZnO_2$ + $H_4SiO_4$; XII – $ZnO_2$ + $H_2SiO_4^{2-}$.

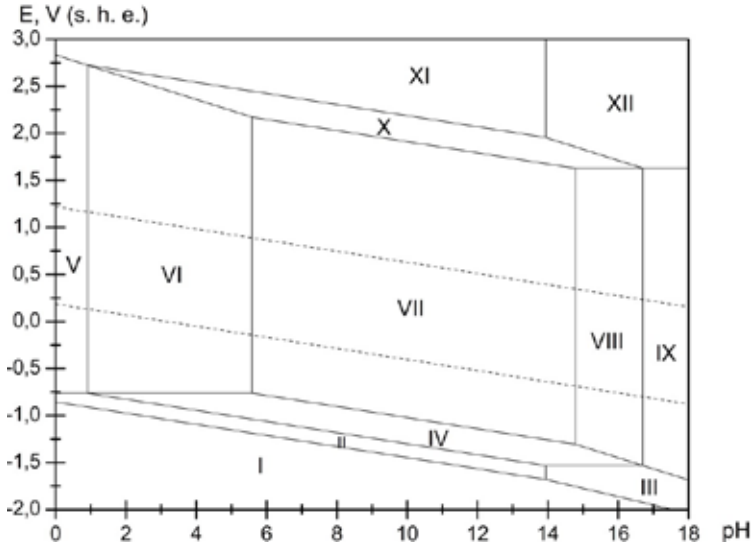


Fig. 9. The potential – pH diagram of Zn – Si – $H_2O$ system at 298 K, air pressure of 1 bar and $a_i$ = 1 mol $l^{-1}$

Zinc silicate has a very wide domain of thermodynamic stability and determines the corrosion behaviour of Zn – Si system. If the silicon content in system is high enough, the protective film consisting of $ZnSiO_3$ would be formed, otherwise zinc oxide ZnO would form the passivity layer.

## Conclusions

The dotted lines on the diagrams (Figures 1 through 9) mark the potentials of hydrogen and oxygen electrodes. The area between these lines depicts the domain of electrochemical stability of water, which is of most interest to researchers. Thermodynamic calculations show that high corrosion resistance of transition metals silicides and metal-silicon alloys in this area is related with formation of the protective films consisting of metals silicates on their surface. These films are much stable in chemical and electrochemical term than films from simple metal oxides. Therefore, silicon reveals good influence on the corrosion resistance of 3d-metals.

The usage of thermodynamic modelling of corrosion properties is not limited to binary systems. It is the powerful instrument that can complement the results of experiments and broaden the knowledge about corrosion-electrochemical behaviour of multicomponent silicon-containing alloys like siliceous bronzes and brasses.

## References

1. Shein A.B. *Elektrokhimiya silitcidov i germanidov perekhodnykh metallov* [Electrochemistry of silicides and germanides of transition metals], Perm State University, *2009.*

2. Tyurin A.G. *Termodimamika khimicheskoi i elektrokhimicheskoi ustoichivosti tverdykh splavov zheleza, khroma i nikelya* [Thermodynamics of chemical and electrochemical stability of solid alloys of iron, chromium and nickel], Chelyabinsk State University, *2011.*

3. Pourbaix M. *Atlas of Electrochemical Equilibria in Aqueous Solutions*. Pergamon Press Ltd., Oxford, *1966*.

4. *Diagrammy sostoyaniya dvoinykh metallicheskikh sistem* [Phase diagrams of binary metallic systems]. In 3 volumes. Edited by Lyakishev N. P., Mashinostroyeniye, Moscow, *1996 – 2000*.

5. Lukashenko G.M., Polotskaya R.I., Sidorko V.R. Thermodynamic properties of scandium, lanthanum, neodymium and gadolinium silicides and germanides // *Journal of Alloys and Compounds*, *1992*, 179(1 – 2), 299 – 305.

6. Horovitz C.T. *Scandium. Its Occurrence, Chemistry, Physics, Metallurgy, Biology and Technology*. Elsevier, *1975*.

7. Hong Z., Cheng L., Zhang L., Wang Y. Water Vapor Corrosion Behavior of Scandium Silicates at 1400 ºC // *Journal of American Ceramic Society*, 2009, 92(1), 193 – 196.

8. Tardy Y., Garrels R.M. Prediction of Gibbs energies of formation–I. Relationships among Gibbs energies of formation of hydroxides, oxides and aqueous ions // *Geochimica et Cosmochimica Acta*, *1976*, 40(9), 1051 – 1056.

9. Tardy Y., Garrels R.M. Prediction of Gibbs energies of formation of compounds from the elements–II. Monovalent and divalent metal silicates // *Geochimica et Cosmochimica Acta*, *1977*, 41(1), 87–92.

10. Travers J.G., Dellien I., Hepler L.G. Scandium: Thermodynamic properties, chemical equilibria, and standard potentials // *Thermochimica Acta*, *1976*, 15(1), 89 – 104.

11. Korosteleva E.N., Pribytkov G.A., Gurskikh A.V. Bulk changes and structurization in solid-phase sintering of titanium–silicon powder mixtures // *Powder Metallurgy and Metal Ceramics*, *2009*, 48(1 – 2), 8 – 12.

12. Liang Z., Dai X., Middleton H. Effect of silicon on corrosion resistance of Ti–Si alloys // *Materials Science and Engineering B*, *2011*, 176(1), 79 – 86.

13. Bandyopadhyay D. The Ti-Si-C system (Titanium-Silicon-Carbon) // *Journal of Phase Equilibria and Diffusion*, *2004*, 25(5), 415 – 420.

14. Yoshikawa T., Morita K., Kawanishi S., Tanaka T. Thermodynamics of impurity elements in solid silicon // *Journal of Alloys and Compounds*, *2010*, 490(1 – 2), 31 – 41.

15. Vahlas C., Shevalier P.Y., Blanquet E. A thermodynamic evaluation of four Si-M (M = Mo, Ta, Ti, W) binary systems // *CALPHAD*, *1989*, 13(3), 273 – 292.

16. Ricker R.W., Hummel F.A. Reactions in the System $TiO_2$–$SiO_2$; Revision of the Phase Diagram // *Journal of the American Ceramic Society*, *1951*, 34(9), 271 – 279.

17. Thermal Constants of Substances: database. URL: < http://www.chem.msu.su/cgibin/tkv.pl?show=welcome.html >.

18. Cotton F., Wilkinson G. *Advanced Inorganic Chemistry. Third Edition*. New York – London – Sydney–Toronto: John Wiley & Sons. *1972*.

19. Nikolaychuk P.A., Tyurin A.G. Termodinamika khimicheskoy i elektrokhimicheskoy ustoychivosti splavov sistemy Ti – Si [Thermodynamics of chemical and electrochemical stability of Ti – Si system alloys] // *Butlerovskiye Soobshcheniya, 2011*, 24(2), 77 – 87.

20. Gokhale A.B., Abbaschian G.J. The Mo-Si (Molybdenum-Silicon) system // *Journal of Phase Equilibria*, *1991*, 12(4), 493 – 498.

21. Tytko K.-H., Glemser O. Isopolymolybdates and Isopolytungstates // *Advances in Inorganic Chemistry and Radiochemistry*, *1976*, 19, 239 – 315.

22. Mahadevaiah N., Venkataramani B., Jai B., Prakash S. Restrictive Entry of Aqueous Molybdate Species into Surfactant Modified Montmorillonite – A Breakthrough Curve Study // *Chemistry of Materials*, *2007*, 19(18), 4606 – 4612.

23. Keullks G.W., Hall J.L., Chellian D., Suzuki K. The catalytic oxidation of propylene: IV. Preparation and characterization of α-bismuth molybdate // *Journal of Catalysis*, *1974*, 34(1), 79 – 97.

24. Sibirkin A.A., Zamyatin O.A., Churbanov M.F. Vzaimnoye prevrashcheniye izopolisoyedineniy molibdena (VI) v vodnom rastvore [Mutual transformation of isopolycompounds of molybdenum (VI) in aqueous solution] // *Vestnik Nizhegorodskogo universiteta imeni N. I. Lobachevskogo*, *2008*, 5, 45 – 51.

25. JANAF Thermochemical Tables. Third Edition // *Journal of Physical and Chemical Reference Data*, *1985*, 14, Supplement. 1.

26. Lee J.B. Elevated Temperature Potential-pH Diagrams for the Cr-$H_2O$, Ti-$H_2O$, Mo-$H_2O$, and Pt-$H_2O$ Systems // *Corrosion, 1981*, 37(8), 467 – 481.

27. Nikolaychuk P.A., Tyurin A.G. Utochnyonnaya diagramma Purbe dlya molibdena [The revised Pourbaix diagram for molybdenum] // *Butlerovskiye Soobshcheniya, 2011*, 24(2), 101 – 105.

28. Nikolaychuk P.A., Tyurin A.G. Termodinamika khimicheskoy i elektrokhimicheskoy ustoychivosti splavov sistemy Mo – Si [Thermodynamics of chemical and electrochemical stability of Mo – Si system alloys] // *Butlerovskiye Soobshcheniya, 2011*, 24(2), 95 – 100.

29. Eremenko V.N. et al. *Fizicheskaya khimiya neorganicheskikh materialov* [Physical chemistry of inorganic materials]: in 3 volumes. Vol. 1. *Termodinamika intermetallidov i fazovye ravnovesiya v metallicheskikh sistemakh* [Thermodynamics of intermetallides and phase equilibria in metallic systems], Naukova Dumka, Kiev, *1988*.

30. Nikolaychuk P.A., Shalyapina T.I., Tyurin A.G., Mosunova T.V. Termodinamika khimicheskoy i elektrokhimicheskoy ustoychivosti splavov sistemy Mn – Si [Thermodynamics of chemical and electrochemical stability of Mn – Si system alloys] // *Vestnik Yuzhno-Ural'skogo gosudarstvennogo universiteta. Seriya "Khimiya"*, *2010*, 4, 31(207), 72 – 82.

31. Chakraborti N., Lukas H.L. Calculation and optimization of the Mn-Si phase diagram // *CALPHAD*, *1989*, 13(3), 293 – 300.

32. Chevalier P.-Y., Fisher E., Rivet A. A Thermodynamic Evolution of the Mn–Si System // *CALPHAD*, *1995*, 19(1), 57 – 68.

33. Miettinen J. Thermodynamic description of the Cu–Mn–Si system in the copper-rich corner // *CALPHAD*, *2003*, 27(4), 395 – 401.

34. Glasser F.P. The system MnO-$SiO_2$ // *American Journal of Science*, *1958*, 256(6), 398 – 412.

35. Huang J.–H., Rosén E. Determination of Gibbs free energies of formation for the silicates $MnSiO_3$, $Mn_2SiO_4$ and $Mn_7SiO_{12}$ in the temperature range 1000–1350 K by solid state emf measurements // *Physics and Chemistry of Minerals*, *1994*, 21(4), 228 – 233.

36. Paschen S., Felder E., Chernikov M.A., Degiorgi L., Schwer H., Ott H.R., Young D.P., Sarrao J.L., Fisk Z. Low-temperature transport, thermodynamic, and optical properties of FeSi // *Physical Review B*, *1997*, 56(20), 12916 – 12930.

37. Lin J.–F., Heinz D. L., Campbell A. J., Devine J. M., Shen G. Iron-Silicon Alloy in Earth's Core? // *Science*, *2002*, 295(5553), 313 – 315.

38. Lau S. S., Feng J. S.-Y., Olowolafe J. O., Nicolet M.-A. Iron silicide thin film formation at low temperatures // *Thin Solid Films*, *1975*, 25(2), 415 – 422.

39. Hu J., Odom T. W. and Lieber C. M. Chemistry and Physics in One Dimension: Synthesis and Properties of Nanowires and Nanotubes // *Accounts of Chemical Research*, *1999*, 32(5), 435 – 445.

40. Patrin G. S., Beletskiĭ V. V., Velikanov D. A., Bayukov O. A., Vershinin V. V., Zakieva O. V., Isaeva T. N. Nonstoichiometry and low-temperature magnetic properties of FeSi crystals // *Physics of the Solid State*, *2006*, 48(4), 700 – 704.

41. Gude A., Mehrer H. Diffusion in the $D0_3$-type intermetallic phase $Fe_3Si$ // *Philosophical Magazine A*, *1997*, 76(1), 1 – 29.

42. Kaufman L. Coupled phase diagrams and thermochemical data for transition metal binary systems-VI // *CALPHAD*, *1979*, 3(1), 45 – 76.

43. Lacaze J., Sundman B. An assessment of the Fe-C-Si system // *Metallurgical and Materials Transactions A*, *1991*, 22(10), 2211 – 2223.

44. Lee B.-J., Lee S. K., Lee D. N. Formulation of the A2/B2/$D0_3$ atomic ordering energy and a thermodynamic analysis of the Fe-Si system // *CALPHAD*, *1987*, 11(3), 253 – 270.

45. Acker J., Bohmhammel K., van der Berg G. J. K., van Miltenburg J. C., Kloc C. Thermodynamic properties of iron silicides FeSi and α-$FeSi_2$ // *Journal of Chemical Termodynamics*, *1999*, 31(12), 1523 – 1536.

46. Navrotsky A. Thermodynamics of formation of the silicates and germanates of some divalent transition metals and of magnesium // *Journal of Inorganic and Nuclear Chemistry*, *1971*, 33, 4035–4050.

47. Fabrichnaya O. B., Sundman B. The assessment of thermodynamic parameters in the Fe–O and Fe–Si–O systems // *Geochimica et CosmochimicaActa*, *1997*, 61(21), 4539 – 4555.

48. Lykasov A. A., Kimyashov A. A. Usloviya fazovykh ravnovesiy v sisteme Fe – Si – O v intervale temperatur 1100 – 1300 K [The features of phase equilibria in Fe – Si – O system in temperature range of 1100 – 1300 K] // *Butlerovskiye Soobshcheniya*, *2010*, 21(7), 42 – 49.

49. Charette G. G., Flengas S. N. Thermodynamic Properties of the Oxides of Fe, Ni, Pb, Cu, and Mn, by EMF Measurements // *Journal of Electrochemical Society*, *1968*, 115(8), 796 – 804.

50. Jacobs M. H. G., de Jong B. H. W. S., Oonk H. A. J. The Gibbs energy formulation of α, γ, and liquid $Fe_2SiO_4$ using Grover, Getting, and Kennedy's empirical relation between volume and bulk modulus // *Geochimica et Cosmochimica Acta*, *2001*, 65(22), 4231 – 4242.

51. Yong W., Dachs E., Withers A. C., Essene E. J. Heat capacity of γ-$Fe_2SiO_4$ between 5 and 303 K and derived thermodynamic properties // *Physical Chemistry of Minerals*, *2007*, 34(2), 121 – 127.

52. Dark A. M., Wei G., Cantor B. The oxidation behaviour of some cobalt-based amorphous alloys // *Materials Science and Engineering B*, *1988*, 99(1 – 2), 533 – 537.

53. Soon-Don C. Thermodynamic analysis of the Co-Si system // *CALPHAD*, *1992*, 16(2), 151 – 159.

54. Tyurin A. G., Mosunova T. V., Nikolaychuk P. A. Termodinamika khimicheskoy i elektrokhimicheskoy ustoychivosti silitcidov kobal'ta [Thermodynamics of chemical and electrochemical stability of cobalt silicides] // *Vestnik Yuzhno-Ural'skogo gosudarstvennogo universiteta. Seriya "Khimiya"*, *2010*, 3, 11(187), 52 – 60.

55. Chen M., Hallstedt B., Gauckler L. J. Thermodynamic assessment of the Co-O system // *Journal of Phase Equilibria*, *2003*, 24(3), 212 – 227.

56. Navrotsky A., Pinchovski F. S., Akimoto S.-I. Calorimetric study of the stability of high pressure phases in the systems CoO–$SiO_2$ and "FeO"–$SiO_2$, and calculation of phase diagrams in MO–$SiO_2$ systems // *Physics of the Earth and Planetary Interiors*, *1979*, 19(4), 275 – 292.

57. Lindholm M., Sundman B. A thermodynamic evaluation of the nickel-silicon system // *Metallurgical and Materials Transactions A*, *1996*, 27(10), 2897 – 2903.

58. Lee P. S., Mangelinck D., Pey K. L., Ding J., Dai J. Y., Ho C. S., See A. On the Ni–Si phase transformation with/without native oxide // *Microelectronic Engineering*, *2000*, 51 – 52, 583 – 594.

59. Tokunaga T., Nishio K., Ohtani H., Hasebe M. Thermodynamic assessment of the Ni–Si system by incorporating ab initio energetic calculations into the CALPHAD approach // *CALPHAD*, *2003*, 27(2), 161 – 168.

60. Yuan X., Zhang L., Du Y., Xiong W., Tang Y., Wang A., Liu S. A new approach to establish both stable and metastable phase equilibria for fcc ordered/disordered phase transition: application to the Al–Ni and Ni–Si systems // *Materials Chemistry and Physics*, *2012*, 135(1), 94 – 105.

61. Acker J., Bohmhammel K. Optimization of thermodynamic data of the Ni–Si system // *Thermochimica Acta*, *1999*, 337(1 – 2), 187 – 193.

62. Ansara I., Sundman B., Willemin P. Thermodynamic modeling of ordered phases in the Ni–Al system // *Acta Metallurgica*, *1988*, 36(4), 977 – 982.

63. Sundman B., Ågren J. A regular solution model for phases with several components and sublattices, suitable for computer applications // *Journal of Physical Chemistry of Solids*, *1981*, 42(4), 297 – 301.

64. Nikolaychuk P. A., Tyurin A. G. Thermodynamic assessment of chemical and electrochemical stability of nickel–silicon system alloys // *Corrosion Science*, *2013*, 73, 237 – 244.

65. Morachevskiy A. G. *Termodinamika sistemy nikel' – kislorod* [Thermodynamics of nickel – oxygen system]: in Morachevskiy, A.G., Tsemekhman, L. Sh., Tsymbulov, L.B. *Termodinamika sistem i protsessov v metallurgii nikelya i medi* [Thermodynamics of systems and processes in metallurgy of nickel and copper]. St. Petersburg: Izdatel'stvo Politekhnicheskogo Universiteta, *2008*. Issue 12.

66. Zeng K., Klassen T., Oelerich W., Bormann R. Thermodynamics of the Ni–H system // *Journal of Alloys and Compounds*, *1999*, 283(1 – 2), 151 – 161.

67. Markos'yan G. N., Sirota D. S., Pchel'nikov A. P. Corrosion of Hydrides of Nickel and Cu30Ni Alloy in Oxygen Containing Solutions // *Protection of Metals*, *2005*, 41(4), 358 – 362.

68. Baranowski B., Bocheńska K. The Free Energy and Entropy of Formation of Nickel hydride // *Zeitschrift für Physikalische Chemie. Neue Folge*, *1965*, 45(3 – 4), 140 – 152.

69. Yan X., Chang Y. A. A thermodynamic analysis of the Cu–Si system // *Journal of Alloys and Compounds*, *2000*, 308(1 – 2), 221 – 229.

70. Nikolaychuk P. A., Tyurin A. G. Termodinamika khimicheskoy i elektrokhimicheskoy ustoychivosti splavov sistemy Cu – Si [Thermodynamics of chemical and electrochemical stability of Cu – Si system alloys] // *Butlerovskiye Soobshcheniya, 2011*, 24(2), 88 – 94.

71. Moiseev G. K., Vatolin N. A. Estimation of the thermochemical properties and stability of $Cu_2O_3$ // *Russian Journal of Physical Chemistry A*, *1997*, 71(3), 335 – 337.

72. Funk J. E., Reinstrom R. M. Energy Requirements in Production of Hydrogen from Water // *Industrial & Engineering Chemistry. Process Design and Development*, *1966*, 5(3), 336 – 342.

73. Vaškelis A., Juškėnas R., Jačiauskienė J. Copper hydride formation in the electroless copper plating process: *in situ* X-ray diffraction evidence and electrochemical study // *Electrochimica Acta*, *1998*, 43(9), 1061 – 1066.

74. Korzhavyi P., Soroka I., Boman M., Johansson B. Thermodynamics of Stable and Metastable Cu-O-H Compounds // *Solid State Phenomena*, *2011*, 172 – 174, 973 – 978.

75. Burtovyy R., Włosewicz D., Czopnik A., Tkacz M. Heat capacity of copper hydride // *Thermochimica Acta*, *2003*, 400(1 – 2), 121 – 129.

76. Tkacz M., Burtovyy R. Decomposition of the hexagonal copper hydride at high pressure // *Solid State Communications*, *2004*, 132(1), 37 – 41.

77. Wriedt H. A. The O−Zn (Oxygen-Zinc) system // *Bulletin of Alloy Phase Diagrams*, *1987*, 8(2), 166 – 176.

78. Jak E., Hayes P. C., Degterov S., Pelton A. D., Wu P. Thermodynamic optimization of the systems PbO-$SiO_2$, PbO-ZnO, ZnO-$SiO_2$ and PbO-ZnO-$SiO_2$ // *Metallurgical and Materials Transaction B*, *1997*, 28(6), 1011 – 1018.

79. Pankratz L. B., Stuve J. M., Gokcen M. A. *Thermodynamic data for mineral technology: handbook //* Bureau of Mines USA, *1984*.

80. Nikolaychuk P. A., Tyurin A. G. Thermodynamic evaluation of corrosion-electrochemical behaviour of silicon brass CuZn17Si3 // *Inorganic Materials*, *2013*, 49(5), 457 – 467.